TRENDS IN SCIENCES 2026; 23(2): 11487
https://doi.org/10.48048/tis.2026.11487
RESEARCH ARTICLE

Heavy-Quark Spin Symmetry Violation Effects in Charmed Baryon Production

Nantana Monkata[1], Prin Sawasdipol[1], Nongnapat Ponkhuha[1], Ratirat Suntharawirat[1], Ahmad Jafar Arifi[2,3] and Daris Samart[1,*]

[1]*Khon Kaen Particle Physics and Cosmology Theory Group, Department of Physics, Faculty of Science, Khon Kaen University, Khon Kaen 40002, Thailand*
[2]*Advanced Science Research Center, Japan Atomic Energy Agency, Ibaraki 3191195, Japan*
[3]*Research Center for Nuclear Physics, The University of Osaka, Osaka 5670047, Japan*

([*]Corresponding author's e-mail: darisa@kku.ac.th)

Received: 3 August 2025, Revised: 16 September 2025, Accepted: 2 October 2025, Published: 10 November 2025

Abstract

In this work, we investigate an effective Lagrangian that describes the interactions between D mesons, charmed baryons (Y_c) and nucleons within the framework of Heavy-Quark Spin Symmetry (HQSS). Using the super-multiplet formalism, we systematically construct the three-point interaction terms. As a result, by considering the minimal sets of the effective Lagrangian in the HQSS construction, there are two effective Lagrangians that are invariant under HQSS whereas we find two minimum terms of the Lagrangian that violate the HQSS transformation. To reveal the phenomenological consequences of HQSS-breaking pattern, we compute the differential cross-sections for exclusive charmed baryon pair production in proton-antiproton collisions, $p\bar{p} \to Y_c \bar{Y}_{c\prime}$, with $Y_c, Y_{c\prime} \in \{\Lambda_c, \Sigma_c, \Sigma_c^*\}$. We demonstrate that the production rates of these channels can be used as a sensitive probe of the HQSS-violating dynamics. Our framework provides predictions for these observables, which are of crucial importance for the upcoming PANDA experiment at the Facility for Antiproton and Ion Research (FAIR).

Keywords: Charmed baryon production, Heavy-Quark Spin Symmetry, Effective Lagrangian

Introduction

One of the challenging questions in particle physics is how strong interactions bind quarks and gluons as described by the non-abelian gauge group $SU(3)$, as is widely known quantum chromodynamics (QCD). At high energies, it is well-defined through perturbation theory due to the interaction weakening with the small couplings. However, non-perturbative QCD becomes strongly coupled and ambiguous at lower energies like a phenomenon known as color confinement. To address the questions, the study of heavy hadrons with a charm quark exhibits distinctive properties that provide valuable insight into QCD.

Charmed baryon states were initially identified in 1975 during interactions with neutrinos [1]. Since then, various facilities such as CLEO [2], BABAR [3,4], Belle [5-7], LHCb collaborations [8,9] have observed various hadrons. Several studies have calculated cross-sections for the production of $p\bar{p} \to \Lambda_c \bar{\Lambda}_c$. The Quark-Gluon String Model (QGSM) and Regge approach were applied [10-15]. The effective Lagrangian model was calculated [16,17] within the sum of the t-channel D^0 and D^{0*} meson-exchange processes. In previous studies, the production varies depending on the model used and there is no agreement on the best way to describe this reaction.

Heavy-quark spin symmetry (HQSS) plays a significant role in understanding of low-energy strong interactions and the classification of the heavy-light hadronic spectrum including the dynamics charm baryons

as studied [18-22]. In the infinite heavy-quark mass limit ($m \to \infty$), the degrees of freedom (DOF) associated with the heavy quark decouple from those of the light quark [23-25]. Note that HQSS is valid for on-shell heavy (charm) quarks. However, in the $p\bar{p} \to \Lambda_c\overline{\Lambda}_c$ process, the charm quark is significantly off-shell due to virtual D-meson exchange [26,27]. This leads to HQSS violation. Although experimental hints of this violation exist [19], the phenomenon remains poorly understood and numerous theoretical studies have been undertaken. Some violations were examined in heavy quarkonium decays [19] and minimal effects were found in the two-meson interaction [28]. More importantly, HQSS breaking was employed to investigate the coupling of $Y(4260)$ to $\overline{D}D_1(2420) + c.c.$ within the framework of the $^3P_0$ quark model [29].

Consequently, this work aims to examine the consequences of HQSS and its violations using constraints to evaluate their effects on scattering processes for charm production such as $p\bar{p} \to \Lambda_c\overline{\Lambda}_c, \Sigma_c\overline{\Sigma}_c, \Sigma_c^*\overline{\Sigma}_c^*, \Sigma_c^*\overline{\Sigma}_c, \Sigma_c\overline{\Sigma}_c^*$, $\Sigma_c\overline{\Lambda}_c, \Lambda_c\overline{\Sigma}_c, \Sigma_c^*\overline{\Lambda}_c$ and $\Lambda_c\overline{\Sigma}_c^*$. We construct the *conserving* and *violating* heavy-quark spin symmetry (CHQSS and VHQSS) Lagrangians and estimate various coupling constants by matching terms to the standard $SU(3)$ effective Lagrangian approach, as studied [17], incorporating $SU(4)_f$ symmetry breaking with a deviation of about 20% relative to $SU(3)_f$ symmetry that was derived by $^3P_0$ quark model [30-32]. Ultimately, we aim to provide precise cross-section predictions for beam momenta (p_{Lab}) from threshold to 15 GeV/c for the future $\overline{\mathrm{P}}$ ANDA (antiProton ANihilation at DArmstadt) experiment at the Facility for Antiproton and Ion Research (FAIR), Germany, which focuses on highly accurate spectroscopy of charmed hadrons and their interactions with ordinary matter [33].

The present work is organized as follows: In the section *Formalism*, we set up the conserving and violating HQSS Lagrangians with their implications. In the next section, we compute the scattering amplitudes and the differential cross-sections in our model. In the section Results and discussion, the numerical results of all relevant observables for the charmed baryon productions are presented. Finally, we close this work with discussions and conclusions.

Formalism

Firstly, to construct the super-multiplet fields in CHQSS and VHQSS Lagrangians of D mesons, nucleon and charmed baryons , all relevant symmetries of the effective Lagrangians in the system are considered. The basic building blocks of the charmed baryon productions from $p\bar{p}$ scattering are introduced as

$$N_a,\ \Lambda_{(c)},\ \Sigma_{(c)ab},\ \Sigma^{\mu}_{(c)ab},\ D_a, D_{\mu a}, \tag{1}$$

where the light baryon singlet fields $N_a(J^P = \frac{1}{2}^+)$, charmed baryon singlet fields $\Lambda_{(c)}(J^P = \frac{1}{2}^+)$ and charmed baryon triplet fields $\Sigma_{(c)ab}(J^P = \frac{1}{2}^+)$ and $\Sigma^{\mu}_{(c)ab}(J^P = \frac{3}{2}^+)$. In addition, the Latin indices, $a, b, \cdots = 1,2$ are the fundamental indices of the $SU(2)_f$ symmetry for the super-multiplet heavy-quark hadronic fields in this work. The D mesons fields $D(J^P = 0^+)$ and $D_\mu(J^P = 1^+)$ are pseudoscalar and vector D mesons respectively, they represent forming a doublet. Furthermore, the nucleon, charmed baryons and, D mesons can be explicitly represented in the $SU(2)_f$ space by

$$N_a = \begin{pmatrix} p \\ n \end{pmatrix}_a,\quad \Lambda_{(c)} = \Lambda^+_{(c)},\quad D_a = \begin{pmatrix} D^0 & D^+ \end{pmatrix}_a,\quad D_\mu = \begin{pmatrix} D^0_\mu & D^+_\mu \end{pmatrix}_a, \tag{2}$$

$$\Sigma_{(c)ab} = \begin{pmatrix} \frac{1}{\sqrt{2}}\Sigma_c^+ & \Sigma_c^{++} \\ \Sigma_c^0 & -\frac{1}{\sqrt{2}}\Sigma_c^+ \end{pmatrix}_{ab}, \Sigma^{\mu}_{(c)ab} = \begin{pmatrix} \frac{1}{\sqrt{2}}\Sigma_c^{\mu,+} & \Sigma_c^{\mu,++} \\ \Sigma_c^{\mu,0} & -\frac{1}{\sqrt{2}}\Sigma_c^{\mu,+} \end{pmatrix}_{ab}, \tag{3}$$

In the heavy-quark limit $m_Q \to \infty$, the spin interaction between light and heavy quarks has disappeared. As a consequence, the pseudoscalar and vector D mesons as well as spin-$\frac{1}{2}$ and spin-$\frac{3}{2}$ baryons form degenerate states, which are based on the following super multiplet field [20,23].

$$H_a = \left(\frac{1+v_\alpha\gamma^\alpha}{2}\right)\left(D_{\mu a}\gamma^\mu + i\gamma_5 D_a\right), \tag{4}$$

$$T^{\mu}_{ab} = \frac{1}{\sqrt{3}}(\gamma^\mu + v^\mu)i\gamma_5\left(\frac{1+v_\alpha\gamma^\alpha}{2}\right)\Sigma_{(c)ab} + \left(\frac{1+v_\alpha\gamma^\alpha}{2}\right)\Sigma^{\mu}_{(c)ab} \tag{5}$$

$$T = \left(\frac{1+v_\alpha\gamma^\alpha}{2}\right)\Lambda_{(c)}\,, \tag{6}$$

And their conjugate fields are

$$\bar{H}_a = \gamma_0 H_a^\dagger \gamma_0 \, , \bar{T}_{ab}^\mu = \left(T_{ab}^\mu\right)^\dagger \gamma_0 \, , \bar{T} = (T)^\dagger \gamma_0 \, . \tag{7}$$

These super-multiplet heavy-quark hadronic fields are building blocks for the HQSS Lagrangian. These building blocks obey the following $SU(2)_v$ transformations,

$$H_a \to e^{-i\theta_\alpha S^\alpha} H_a \, , \; \bar{H}_a \to \bar{H}_a e^{i\theta_\alpha S^\alpha} \, , \tag{8}$$

$$T_{ab}^\mu \to e^{-iS_\alpha \theta^\alpha} T_{ab}^\mu \, , \; \bar{T}_{ab}^\mu \to \bar{T}_{ab}^\mu e^{i\theta_\alpha S^\alpha} \, , \tag{9}$$

$$T \to e^{-iS_\alpha \theta^\alpha} T \, , \; \bar{T} \to \bar{T} e^{iS_\alpha \theta^\alpha} \, , \tag{10}$$

where S^α is the heavy quark spin operator. We note The CHQSS and VHQSS Lagrangians presented above indicate that invariance under the spin symmetry group $SU_v(2)$ is preserved only when the Dirac structures are positioned either after the field H or before its conjugate $\bar{H}$ with respect to meson supermultiplets, in a manner analogous to baryon supermultiplets. Specifically, configurations that maintain this invariance under $SU_v(2)$ require that nontrivial Dirac matrices do not precede the fields N_b and N_a, nor follow the fields $\bar{T}_{ab}^\mu$ and $\bar{T}$. It should be noted that the constructions of the CHQSS and VHQSS Lagrangians are regarded as the minimal set. More importantly, the three point interaction Lagrangians of CHQSS and VHQSS were first constructed in this work. Previous studies have not considered charmed baryons, D-mesons and nucleons under HQSS framework but only four-point interaction of charmed baryons, D-mesons, nucleons and $c\bar{c}$-mesons was established [34]. Accordingly, employing the definitions of the supermultiplet heavy-quark fields as outlined in Eqs. (4) - (6), we are able to express the CHQSS and VHQSS Lagrangians explicitly as follows,

$$\mathcal{L}_{\text{CHQSS}} = \; -\frac{1}{\sqrt{3}} c_1 \bar{\Sigma}_{(c)ab} \gamma^\mu D_\mu N + \frac{3}{\sqrt{3}} c_1 \bar{\Sigma}_{(c)ab} i\gamma_5 D_a N + 2c_1 \bar{\Sigma}^\mu_{(c)ab} \gamma_5 D_\mu N \tag{14}$$

that all super-multiplet heavy-quark hadronic fields transform as doublet under $SU(2)_v$ HQSS where as the nucleon field is transformed as a singlet under the $SU(2)_v$ symmetry. The definition of the heavy-quark spin operator and its properties are read,

$$S^\alpha = \tfrac{1}{2}\gamma_5[v, \gamma^\alpha] \, , \; S_\alpha^\dagger \gamma_0 = \gamma_0 S_\alpha \, , \; [v, S_\alpha] = 0 \, , \; [S_\alpha, \gamma_5] = 0 \tag{11}$$

Taking into account for all of the super-multiplet fields of the HQSS, the conserving HQSS (CHQSS) Lagrangian is given by

$$\mathcal{L}_{CHQSS} = c_1 \bar{T}_{ab}^\mu H_a \gamma_\mu \gamma_5 N_b + \text{h.}\, c. + c_2 \bar{T} H_a N_a + \text{h.}\, c. \tag{12}$$

On the other hand, the violating HQSS (VHQSS) Lagrangian is read,

$$\mathcal{L}_{\text{VHQSS}} = \; b_1 \bar{T}_{ab}^\mu \gamma^\nu H_a \gamma_\mu \gamma_\nu \gamma_5 N_b + \text{h.}\, c. + b_2 \bar{T} \gamma^\mu H_a \gamma_\mu N_a + \text{h.}\, c. \tag{13}$$

$$+ c_2 \bar{\Lambda}_{(c)} \gamma^\mu D_{\mu a,+} N + c_2 \bar{\Lambda}_{(c)} i\gamma_5 D_{a,+} N + \text{h. c.}, \tag{15}$$

$$\mathcal{L}_{\text{VHQSS}} = \; \frac{6}{\sqrt{3}} b_1 \bar{\Sigma}_{(c)ab} \gamma^\mu D_\mu N + \frac{12}{\sqrt{3}} b_1 \bar{\Sigma}_{(c)ab} i\gamma_5 D_a N + 4b_1 \bar{\Sigma}^\mu_{(c)ab} \gamma_5 D_\mu N \tag{16}$$

$$+ 2b_2 \bar{\Lambda}_{(c)} \gamma^\mu D_{\mu a,+} N + 4b_2 \bar{\Lambda}_{(c)} i\gamma_5 D_{a,+} N + \text{h. c.}. \tag{17}$$

We obtain the ratios between the conserving coupling constants c_1 and c_2 and the violating couplings b_1 and b_2. The results show that the violating terms are suppressed relative to the conserving ones for pseudoscalar, axial-vector and vector interaction couplings by factors of $c_1/4b_1$, $c_1/2b_1$ and $c_1/6b_2$ for $\Sigma_{(c)}$ and by $c_2/4b_2$ and $c_2/2b_2$ for pseudoscalar and vector interactions in the case of $\Lambda_{(c)}$, respectively. As a result, HQSS significantly reduces the number of independent parameters, leaving only a small set of low-energy constants (LECs) to determine. Since the QCD action depends linearly on the heavy quark mass, the effective Lagrangians in Eqs (12) - (13) reflect an overall scaling with the charm quark mass M_c. Consequently, the couplings introduced previously scale linearly with M_c. With these constraints in place, we can fix the remaining couplings and compute the scattering amplitudes for CHQSS and VHQSS, along with their differential cross sections.

A. Determination of coupling constants (LECs) of the effective lagrangians

Due to the limited experimental data relevant to our study, theoretical estimations are required to determine these LECs. Subsequently, we establish a correspondence between the CHQSS and VHQSS Lagrangians, as presented in Eqs. (14) - (15), by matching their relations with those obtained from the standard SU(3) effective Lagrangian approach, as studied [17]. This enables us to derive the relations between the conserving and violating coupling constants for the vector coupling f as follows,

$$c_1 = -\sqrt{3}f_1, \quad c_2 = f_2 \tag{18}$$

For the violating terms,

$$b_1 = \frac{\sqrt{3}}{6}f_1, \quad b_2 = \frac{f_2}{2} \tag{19}$$

It shows that the vector couplings in the violating terms are suppressed relative to the conserving ones by factors of $1/6$ and $1/2$ for f_1 and f_2, respectively. For the vector ($f_{1,2}$), we found that the $SU(4)_f$ symmetry of the baryon-baryon-meson couplings implies

$$f_1 \equiv f_{DN\Sigma_c} = f_{KN\Sigma}\,, \tag{20}$$
$$f_2 \equiv f_{DN\Lambda_c} = f_{KN\Lambda}\,. \tag{21}$$

However, $SU(4)_f$ symmetry is not a good approximation for combining light and heavy quarks, we consider its breaking in baryon-baryon-meson interactions. Using the $^3P_0$ quark model, symmetry-breaking effects on couplings among heavy baryons, light baryons, and heavy mesons have been demonstrated [31,32]. This provides a reasonable first approximation, with about a 20% deviation from exact $SU(4)_f$ values [30-32]. Thus, the coupling constants (LECs) for D mesons, charmed baryons, and light baryons derived from $SU(4)_f$ symmetry breaking are given by

$$f_1 = -4.182 \pm 0.836, \quad f_2 = 5.11 \pm 1.02 \tag{22}$$

Next, we proceed to calculate the scattering amplitudes by applying these vector coupling values, together with the proportions of conserving and violating terms for pseudoscalar and axial-vector coupling constants.

Scattering ampliudes

In this section, we aim to calculate the differential cross-sections of $p\bar{p} \to \Lambda_c\overline{\Lambda}_c, \Sigma_c\bar{\Sigma}_c, \Sigma_c^*\bar{\Sigma}_c^*, \Sigma_c^*\bar{\Sigma}_c, \Sigma_c\bar{\Sigma}_c^*$, $\Sigma_c\overline{\Lambda}_c, \Lambda_c\bar{\Sigma}_c, \Sigma_c^*\overline{\Lambda}_c$ and $\Lambda_c\bar{\Sigma}_c^*$ processes. For those processes, we will investigate the consequences of the HQSS and its violation effects in the charmed baryon productions and the Feynman diagram of these processes have been shown in **Figure 1** This diagram underlies all channels shown in **Figures 2 - 10**.

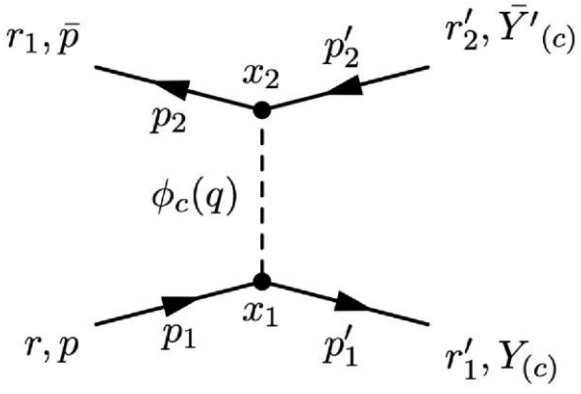

Figure 1 Tree-level diagram for the reactions $p\bar{p} \to Y_c\bar{Y}_c{}'$, where Y_c and $\bar{Y}'_c$ represent charmed baryons. ϕ_c, in the intermediate line, represents the pseudoscalar and vector D mesons, respectively.

A. The scattering amplitudes

According to the Lagrangians in terms of conserving and violating parts in Eqs. (14) - (15), the scattering amplitudes of charmed productions with the exchanges of the pseudoscalar and vector D mesons are written as follows,

Process: $p\bar{p} \to \Lambda_c\bar{\Lambda}_c$

$$\begin{aligned}\mathcal{M}_C &= c_2^2\,\Gamma_{N(P)}\,G(q)\,\Gamma_{\bar{N}(P)} + c_2^2\,\Gamma^{\mu}_{N(V)}\,G_{\mu\nu}(q)\;\Gamma^{\nu}_{\bar{N}(V)}\\ \mathcal{M}_V &= 16b_2^2\,\Gamma_{N(P)}\,G(q)\,\Gamma_{\bar{N}(P)} + 4b_2^2\,\Gamma^{\mu}_{N(V)}\,G_{\mu\nu}(q)\;\Gamma^{\nu}_{\bar{N}(V)}.\end{aligned} \tag{23}$$

Process: $p\bar{p} \to \Sigma_c\bar{\Sigma}_c$

$$\begin{aligned}\mathcal{M}_C &= 3c_1^2\,\Gamma_{N(P)}\,G(q)\,\Gamma_{\bar{N}(P)} + \tfrac{1}{3}c_1^2\,\Gamma^{\mu}_{N(V)}\,G_{\mu\nu}(q)\;\Gamma^{\nu}_{\bar{N}(V)}\\ \mathcal{M}_V &= 48b_1^2\,\Gamma_{N(P)}\,G(q)\,\Gamma_{\bar{N}(P)} + 12b_1^2\,\Gamma^{\mu}_{N(V)}\,G_{\mu\nu}(q)\;\Gamma^{\nu}_{\bar{N}(V)}.\end{aligned} \tag{24}$$

Process: $p\bar{p} \to \Lambda_c\bar{\Sigma}_c$

$$\begin{aligned}\mathcal{M}_C &= \tfrac{3}{\sqrt{3}}c_2c_1\,\Gamma_{N(P)}\,G(q)\,\Gamma_{\bar{N}(P)} - \tfrac{1}{\sqrt{3}}c_2c_1\,\Gamma^{\mu}_{N(V)}\,G_{\mu\nu}(q)\;\Gamma^{\nu}_{\bar{N}(V)}\\ \mathcal{M}_V &= \tfrac{48}{\sqrt{3}}b_2b_1\,\Gamma_{N(P)}\,G(q)\,\Gamma_{\bar{N}(P)} + \tfrac{12}{\sqrt{3}}b_2b_1\,\Gamma^{\mu}_{N(V)}\,G_{\mu\nu}(q)\;\Gamma^{\nu}_{\bar{N}(V)}.\end{aligned} \tag{25}$$

Process: $p\bar{p} \to \Sigma_c\bar{\Lambda}_c$

$$\begin{aligned}\mathcal{M}_C &= \tfrac{3}{\sqrt{3}}c_1c_2\,\Gamma_{N(P)}\,G(q)\,\Gamma_{\bar{N}(P)} - \tfrac{1}{\sqrt{3}}c_1c_2\,\Gamma^{\mu}_{N(V)}\,G_{\mu\nu}(q)\;\Gamma^{\nu}_{\bar{N}(V)}\\ \mathcal{M}_V &= \tfrac{48}{\sqrt{3}}b_1b_2\,\Gamma_{N(P)}\,G(q)\,\Gamma_{\bar{N}(P)} + \tfrac{12}{\sqrt{3}}b_1b_2\,\Gamma^{\mu}_{N(V)}\,G_{\mu\nu}(q)\;\Gamma^{\nu}_{\bar{N}(V)}.\end{aligned} \tag{26}$$

Process: $p\bar{p} \to \Sigma_c^*\bar{\Sigma}_c^*$

$$\begin{aligned}\mathcal{M}_C &= 4c_1^2\,\Gamma^{\mu}_{N(V^*)}\,G_{\mu\nu}(q)\,\Gamma^{\nu}_{\bar{N}(V)}\\ \mathcal{M}_V &= 16b_1^2\,\Gamma^{\mu}_{N(V^*)}\,G_{\mu\nu}(q)\,\Gamma^{\nu}_{\bar{N}(V)}.\end{aligned} \tag{27}$$

Process: $p\bar{p} \to \Lambda_c\bar{\Sigma}_c^*$

$$\begin{aligned}\mathcal{M}_C &= 2c_2c_1\,\Gamma^{\mu}_{N(V)}\,G_{\mu\nu}(q)\,\Gamma^{\nu}_{\bar{N}(V^*)}\\ \mathcal{M}_V &= 8c_2c_1\,\Gamma^{\mu}_{N(V)}\,G_{\mu\nu}(q)\,\Gamma^{\nu}_{\bar{N}(V^*)}.\end{aligned} \tag{28}$$

Process: $p\bar{p} \to \Sigma_c^*\bar{\Lambda}_c$

$$\begin{aligned}\mathcal{M}_C &= 2c_1c_2\,\Gamma^{\mu}_{N(V^*)}\,G_{\mu\nu}(q)\,\Gamma^{\nu}_{\bar{N}(V)}\\ \mathcal{M}_V &= 8c_1c_2\,\Gamma^{\mu}_{N(V^*)}\,G_{\mu\nu}(q)\,\Gamma^{\nu}_{\bar{N}(V)}.\end{aligned} \tag{29}$$

Process: $p\bar{p} \to \Sigma_c^*\bar{\Sigma}_c$

$$\begin{aligned}\mathcal{M}_C &= -\tfrac{2}{\sqrt{3}}c_1^2\,\Gamma^{\mu}_{N(V^*)}\,G_{\mu\nu}(q)\,\Gamma^{\nu}_{\bar{N}(V)}\\ \mathcal{M}_V &= \tfrac{24}{\sqrt{3}}b_1^2\,\Gamma^{\mu}_{N(V^*)}\,G_{\mu\nu}(q)\,\Gamma^{\nu}_{\bar{N}(V)}.\end{aligned} \tag{30}$$

Process: $p\bar{p} \to \Sigma_c\bar{\Sigma}_c^*$

$$\begin{aligned}\mathcal{M}_C &= -\tfrac{2}{\sqrt{3}}c_1^2\,\Gamma^{\mu}_{N(V)}\,G_{\mu\nu}(q)\,\Gamma^{\nu}_{\bar{N}(V^*)}\\ \mathcal{M}_V &= \tfrac{24}{\sqrt{3}}\,\Gamma^{\mu}_{N(V)}\,G_{\mu\nu}(q)\,\Gamma^{\nu}_{\bar{N}(V^*)}.\end{aligned} \tag{31}$$

Here, $\mathcal{M}_C$ and $\mathcal{M}_V$ denote the conserving and violating scattering amplitudes, respectively. The Γ notations appear in the scattering amplitudes above and they are defined by,

$$\begin{aligned}&\Gamma_{N(P)} = \bar{u}_{Y_c}\,i\,\gamma_5\,u_N, \quad \Gamma_{\bar{N}(P)} = -\bar{v}_{\bar{N}}\,i\,\gamma_5\,v_{\bar{Y}_c},\\ &\Gamma^{\mu}_{N(V)} = \bar{u}_{Y_c}\,\gamma^{\mu}\,u_N, \quad \Gamma^{\nu}_{\bar{N}(V)} = -\bar{v}_{\bar{N}}\,\gamma^{\nu}\,v_{\bar{Y}_c},\\ &\Gamma^{\mu}_{\bar{N}(V^*)} = \bar{u}^{\mu}_{Y_c}\,\gamma_5\,u_N, \quad \Gamma^{\nu}_{N(V^*)} = -\bar{v}_{\bar{N}}\,\gamma_5\,v^{\nu}_{\bar{Y}_c},\end{aligned} \tag{32}$$

where $\Gamma_{N(P)}$ and $\Gamma_{N(V)}$ denote the vertices for charmed baryons with spin-$\frac{1}{2}$, while $\Gamma_{N(V^*)}$ represents spin-$\frac{3}{2}$. The Feynman propagators for the pseudoscalar D meson (spin-0) and the vector D meson (spin-1) are defined by:

$$G(q) = \frac{i}{q-m_D^2}, \quad G_{\mu\nu}(q) = \frac{i}{q-m_{D^*}^2}\left(-g_{\mu\nu} + \frac{q_\mu q_\nu}{m_{D^*}^2}\right). \tag{33}$$

B. differential cross-sections

It is well known that a study of the scattering of the composite particles, precisely hadrons needs the form factor to regulate the amplitudes and to describe the internal hadronic structures. In this work, we include phenomenological form factors taken from Ref. [17], whose unknown parameters are determined from experimental data on strangeness production and then extrapolated to charmed baryon production. The form factors used in this work are given by

$$F(t) = a^2\,\frac{\Lambda^4}{\Lambda^4 + \left(t-m_\phi^2\right)^2}, \tag{34}$$

$$F_n(t) = a\left(\frac{\Lambda^2}{\Lambda^2 - t}\right)^n, \quad (n = 1,2) \tag{35}$$

The form factor $F(t)$, with parameters $a = 0.46$ and $\Lambda = 0.63$ GeV. For $F_1(t)$, the parameters are $a = 0.285$ and $\Lambda = 0.7$ GeV, while for $F_2(t)$, the parameters are $a = 0.285$ and $\Lambda = 0.99$ GeV, where a serves as the normalization constant in both cases, with Λ and m_ϕ denoting the cutoff parameter and the mass of the exchanged D-mesons, respectively. The total amplitudes of the reactions $p\bar{p} \to Y_c\bar{Y}_c$ are written as

$$\mathcal{M}_{p\bar{p}\to Y_c\bar{Y}_c'} = \begin{cases} \mathcal{M}_D F_D + \mathcal{M}_{D^*} F_{D^*}, \\ \mathcal{M}_D F_{n,D}^2 + \mathcal{M}_{D^*} F_{n,D^*}^2. \end{cases} \quad (36)$$

The form factors $F_{(D,D^*)}$ are included in the entire amplitude and $F_{n(D,D^*)}$ are multiplied at each vertex, as already mentioned in Eqs. (31) - (32) for the pseudoscalar D-meson (D) and the vector D-meson (D^*). It is common practice to use various functional forms and cutoff values for t-channel form factors [35-37]. The differential cross-sections as a function of t is calculated from

$$\frac{d\sigma}{dt} = \frac{1}{64\pi(p_{cm})^2 s}\langle|\mathcal{M}|^2\rangle. \quad (37)$$

Here, p_{cm} is the relative momentum of p and $\bar{p}$ in the center-of-mass frame, s is the Mandelstam variable. The term $\langle|\mathcal{M}|^2\rangle$ is the spin-averaged and summed amplitude, given by

$$\langle|\mathcal{M}|^2\rangle = \frac{1}{4}\sum_{spin}|\mathcal{M}|^2. \quad (38)$$

where the sum runs over the spins of the final-state particles. After averaging and summing over spins Eq. (35) the interference term vanishes. This is because of the spin averaging eliminates interference between spin configurations. Trace analysis reveals that the interference term would mix D and D^* mesons, which is prohibited by conservation of parity. In this study, the differential cross sections, $d\sigma/dt$, in section *Results and Discussion* are presented as functions of $t_{max} - t$. For a specific energy value, t varies from t_{min} to t_{max} (i.e., $t_{\mathrm{max}} - t$ varies from 0 to $t_{\mathrm{max}} - t_{\mathrm{min}}$). One can write the explicit form of the $t_{\mathrm{max}}^{\mathrm{min}}$ as,

$$t_{\mathrm{max}}^{\mathrm{min}} = m_N^2 + m_{Y_c}^2 - \frac{1}{2s}[s(s + m_{Y_c}^2 - m_{Y_c'}^2) \pm \sqrt{s(s-4m_N^2)(s-(m_{Y_c}+m_{Y_c'})^2)} \times \sqrt{(s-(m_{Y_c}-m_{Y_c'})^2)}]. \quad (39)$$

Results and discussion

In this section, the numerical results of the differential cross-sections, $d\sigma/dt$, are presented as a function of $t - t_{\mathrm{max}}$ for the reaction $p\bar{p} \to Y_c\bar{Y}_c{}'$, evaluated for each form factor at $p_{\mathrm{Lab}} = 15\ \mathrm{GeV/c}$ in **Figures 2 - 10**. Considering the effects of $SU(4)_f$ symmetry breaking with the uncertainty of 20% of the coupling constants described previously, the green bands represent the conserving production, the red bands show the violating parts and the purple bands illustrate the total contributions. The dashed lines represent central values without the $\pm$ 20% uncertainty: The white dashed line corresponds to the conserving contribution, the red dashed line to the violating contribution and the purple dashed line to the total differential cross-section. The graphs appear on band-length scales due to uncertainty. However, several studies reveal that charm production is represented on the band graph and its behavior depends on the theoretical approach [12,38,39].

A. Numerical results of the scattering amplitudes of the $p\bar{p} \to Y_c\bar{Y}_c'$ reactions

In **Figure 2**, our predicted differential cross-sections for $\bar{p}p \to \bar{\Lambda}_c\Lambda_c$ show that violating terms contribute marginally more than conserving terms—about 51 - 53%, depending on the form factor, with exact values of 53.29%, 51.99% and 52.70% for form factors F, F_1 and F_2, while the conserving terms correspond to 46.71%, 48.01% and 47.30%, respectively. The conserving contribution is weaker than the violating one because the coupling strength of the violating term is twice as large as that of the conserving term for the pseudoscalar interaction, as shown in Eqs. (16) - (17), which originate from the CHQSS and VHQSS Lagrangians in Eqs. (14) - (15). These differences influence the scattering amplitudes in Eq. (20).

The tendencies illustrate that the exact value depends on the type of form factor. In **Figures 2(a) - 2(c)**, the total $d\sigma/dt$ follows a similar trend in order of $10^{-3}(F)$,$10^{-1}(F_1)$ and $10^{-2}(F_2)$ $\mu\mathrm{b/GeV^2}$ respectively. The F_2 is, consistent with the findings of Titov and Kampfer [11], about 10^{-2} $\mu\mathrm{b/GeV^2}$ at the excess energy at $t_{\mathrm{max}} - t = 0\ \mathrm{GeV^2}$, which employs a modified Regge model inspired by quark-gluon string dynamics, with unknown parameters determined from independent studies of open strangeness production and $SU(4)_f$ symmetry. Likewise, the results for F are consistent with those reported in Khodjamirian *et al.* [12], which employs Kaidalov's QGSM with Regge poles and strong couplings derived from QCD light-cone sum rules and presents $d\sigma/dt$ as a function of $-t$.

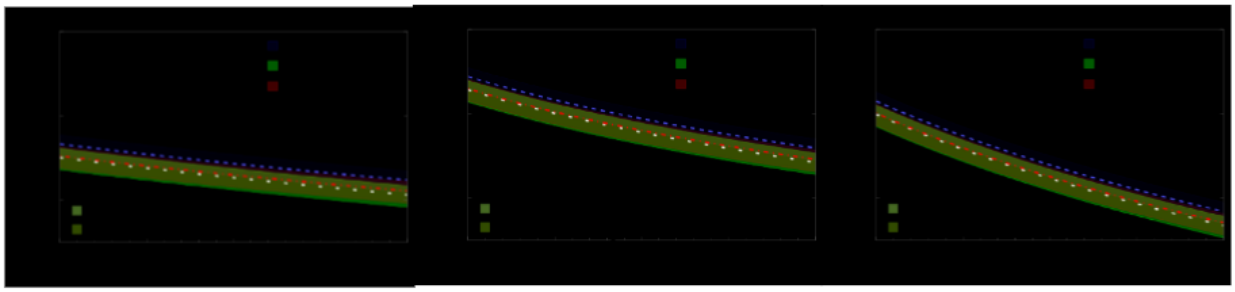

(a) (b) (c)

Figure 2 Differential cross section $d\sigma/dt$ for $\bar{p}p \to \Lambda_c\bar{\Lambda}_c$ at $p_{\text{lab}} = 15\text{GeV}/c$, plotted versus $t_{\text{max}} - t$ (GeV^2). Panels (a)-(c) use the three vertex form factors F, F_1, F_2 defined in Eqs. (31) - (32); bands reflect $\pm 20\%$ SU(4)-breaking variations of the couplings (green: Conserving; red: Violating; purple: Total; dashed lines are central values).

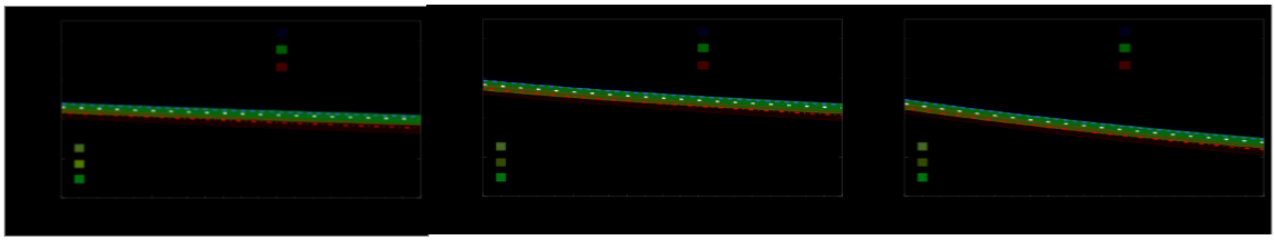

(a) (b) (c)

Figure 3 Differential cross section $d\sigma/dt$ for $\bar{p}p \to \Sigma_c\bar{\Sigma}_c$ at $p_{\text{lab}} = 15\text{GeV}/c$, shown versus $t_{\text{max}} - t$ for F, F_1, F_2. Bands and dashed lines have the same meaning as in **Figure 2**. Here the conserving part dominates (about 66%), consistent with the presence of heavy-quark spin partners in the final state; typical magnitudes lie between $10^{-3} - 10^{-1}\mu$ b/GeV^2 depending on the form factor.

In **Figure 3** the differential cross-section for $p\bar{p} \to \Sigma_c\bar{\Sigma}_c$ is shown. Most of the production rate is dominated by the conserving terms, contributing about $65\% - 68\%$, which are 68.64%, 64.07% and 65.98% for the respective form factors, while the violating contributions are 31.36%, 35.93%, and 34.02%, respectively. We obtain that the total $d\sigma/dt$ is around 10^{-3} μb/GeV^2 (F and F_2) and 10^{-2} μb/GeV^2 (F_1). These contributions are lower than those for $p\bar{p} \to \Lambda_c\bar{\Lambda}_c$ by about one order of magnitude. More importantly, the F and F_2 constraints are in close agreement with the studies [11,12]. Nevertheless, the impact of $F_2(t)$ diminishes at higher values of $t_{\text{max}} - t$ due to its form factor, where the squared smaller cutoff Λ (0.99 GeV) enhances suppression, even though it uses the same parameter a (0.285) as $F_1(t)$.

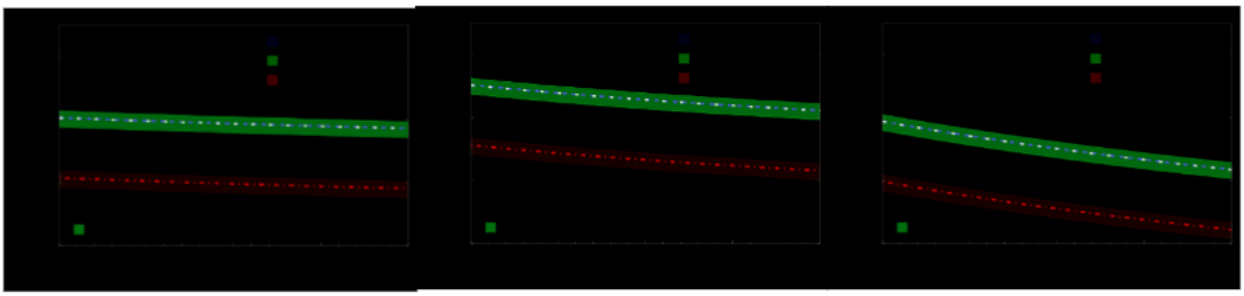

(a) (b) (c)

Figure 4 Differential cross section $d\sigma/dt$ for $\bar{p}p \to \Sigma_c^*\bar{\Sigma}_c^*$ at $p_{\text{lab}} = 15\text{GeV}/c$ versus $t_{\max} - t$ for F, F_1, F_2. The conserving contribution is overwhelmingly dominant ($\simeq 98.8\%$); F_2 shows the strongest high- t suppression, with the violating term reaching $\sim 10^{-8}\mu\ \text{b/GeV}^2$ near $t_{\max} - t = 2\text{GeV}^2$.

Currently, the production rates of $\Sigma_c^*\bar{\Sigma}_c^*$ have not been extensively investigated, including in experiments. Since we are performing calculations at high beam momenta $p_{\text{Lab}} = 15$ GeV, this leads us to further explore the spectroscopy of this production and its interactions in experiments. Our results for $p\bar{p} \to \Sigma_c^*\bar{\Sigma}_c^*$ are shown in **Figure 4**. These contributions primarily come from the conserving terms is estimated to be about 98.78%, with the violation being 1.22% for each form factor. The orders of the conserving rates are 10^{-4} (F), 10^{-3} (F_1) and 10^{-4} (F_2) $\mu\text{b/GeV}^2$, while violation terms range from $10^{-6}, 10^{-5}$ and 10^{-6} $\mu\text{b/GeV}^2$ respectively. We clearly observe that the F_2 becomes more suppressed at the excess energy $t_{\max} - t = 2$ GeV^2, reaching 10^{-8} $\mu\text{b/GeV}^2$, in agreement with previous calculations.

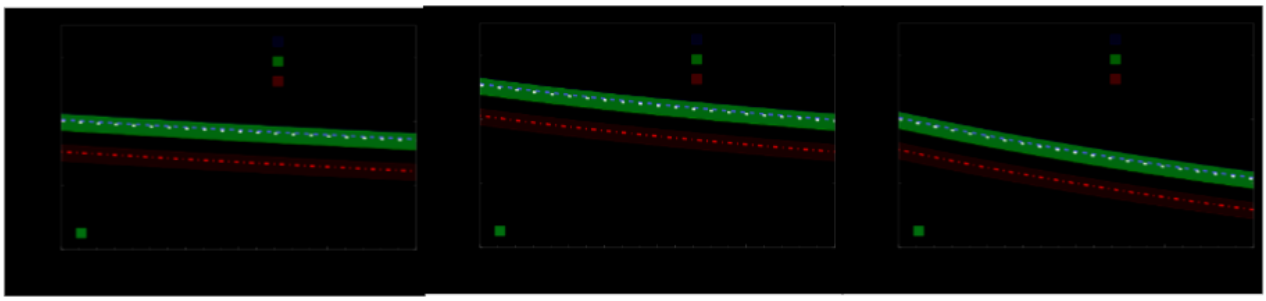

(a) (b) (c)

Figure 5 Differential cross section $d\sigma/dt$ for $\bar{p}p \to \Sigma_c^*\bar{\Sigma}_c$ at $p_{\text{lab}} = 15\text{GeV}/c$ versus $t_{\max} - t$ for F, F_1, F_2. The conserving piece remains dominant at $\sim 90\%$, with totals ranging from $10^{-5} - 10^{-3}\mu\ \text{b/GeV}^2$ (form-factor dependent).

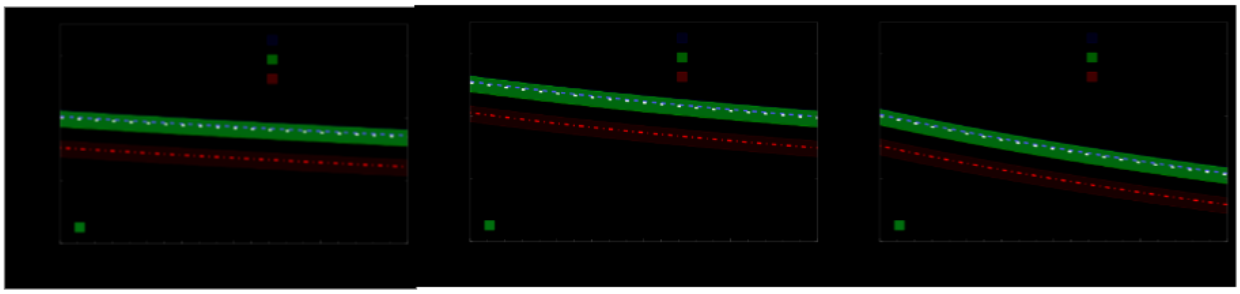

(a) (b) (c)

Figure 6 Differential cross section $d\sigma/dt$ for $\bar{p}p \to \Sigma_c\bar{\Sigma}_c^*$ (charge-conjugate ordering of **Figure 5**) at $p_{\text{lab}} = 15\text{GeV}/c$ versus $t_{\text{max}} - t$ for F, F_1, F_2. As in **Figure 5**, the conserving term contributes ~9%; the qualitative t-dependence and band overlap closely mirror the $\Sigma_c^*\bar{\Sigma}_c$ case.

Shown in **Figure 5** are the results for $p\bar{p} \to \Sigma_c^*\bar{\Sigma}_c$, which has not been widely studied either, similar to $\Sigma_c^*\bar{\Sigma}_c^*$. We found that the conserving terms still play a dominant role, with approximately 90%. The total $d\sigma/dt$ varies in the range 10^{-4}–10^{-3} $\mu\text{b}/\text{GeV}^2$, which are 10^{-4} $\mu\text{b}/\text{GeV}^2$ (F and F_2) and 10^{-3} $\mu\text{b}/\text{GeV}^2$ (F_1). Notably, the conserving contributions remain similar to those for $\Sigma_c^*\bar{\Sigma}_c^*$, whereas the violating contributions differ, being higher by about one order of magnitude. When compared with $\Sigma_c\bar{\Sigma}_c^*$, a similar trend is clearly observed, as shown in **Figure 6**.

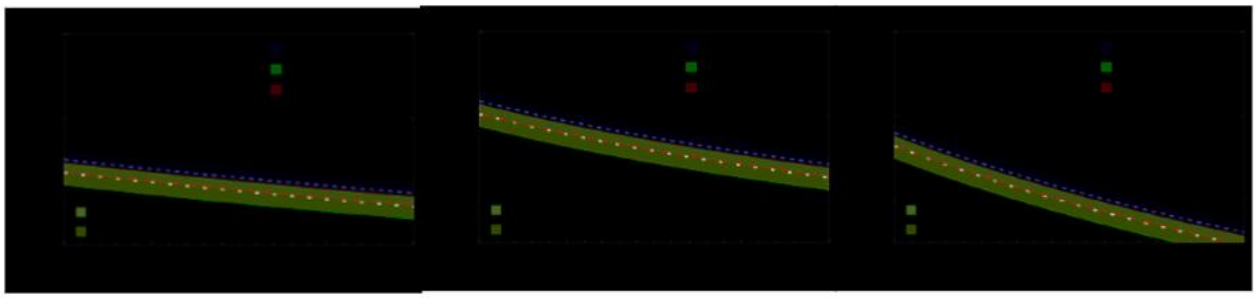

(a) (b) (c)

Figure 7 Differential cross section $d\sigma/dt$ for the mixed channel $\bar{p}p \to \Lambda_c\bar{\Sigma}_c$ at $p_{\text{lab}} = 15\text{GeV}/c$, shown versus $t_{\text{max}} - t$ for F, F_1, F_2. In this non-partner final state, the conserving and violating pieces are comparable (violating is larger by roughly 2% - 4% across the three form factors), producing broad, partially overlapping bands.

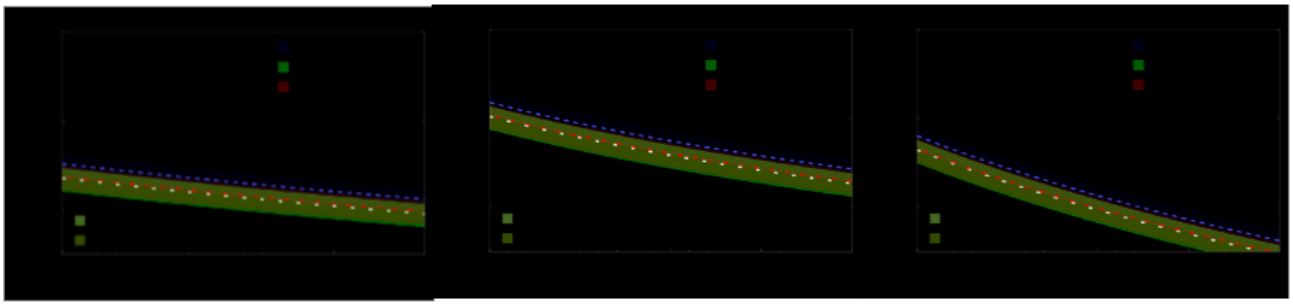

(a) (b) (c)

Figure 8 Differential cross section $d\sigma/dt$ for $\bar{p}p \to \Sigma_c\bar{\Lambda}_c$ (charge-conjugate ordering of **Figure 7**) at $p_{\text{lab}} = 15\ \text{GeV}/c$, shown versus $t_{\text{max}} - t$ for F, F_1, F_2. The conserving and violating contributions come out nearly equal, with a slight excess on the violating side; the overall scale sits between those of the pure $\Lambda_c\bar{\Lambda}_c$ and $\Sigma_c\bar{\Sigma}_c$ channels.

The $\Sigma_c\overline{\Lambda}_c$ channel, as illustrated in **Figure 8**. This channel exhibits stronger interactions and fits better with simpler theoretical models than $\Lambda_c\bar{\Sigma}_c$. However, to fully understand the $p\bar{p}$ annihilation process, it is important to study both final states. Our prediction shows that the HQSS-conserving contribution is slightly lower than the violating one, similar to the case of $\Lambda_c\overline{\Lambda}_c$, where the pseudoscalar coupling strength for the violating term is larger, with a ratio of 4:3 compared to the conserving term. The $\Lambda_c\bar{\Sigma}_c$ production, as observed in **Figure 7**, reveals about 48% for conserving and 51% for violating respectively. A similar trend is observed in the $\Sigma_c\overline{\Lambda}_c$, with around 47% contribution from the conserving term and 52% from the violating one.

The total $d\sigma/dt$ falls in the range of 10^{-3} – $10^{-2}\ \mu\text{b}/\text{GeV}^2$, which are $10^{-3}\ \mu\text{b}/\text{GeV}^2$ (F) and $10^{-2}\ \mu\text{b}/\text{GeV}^2$ (F_1) and almost $10^{-2}\ \mu\text{b}/\text{GeV}^2$ (F_2), these minimally above those for the $\Sigma_c\bar{\Sigma}_c$ channel but remain under those for $\Lambda_c\overline{\Lambda}_c$. Furthermore, the F_2 constrain found to be agree with Titov and Kampfer [11] and those for F align with Khodjamirian *et al.* [12]. The observed similarity arises not only from the pseudoscalar coupling strengths but also from the squared amplitudes of the pseudoscalar and vector interactions, as uncovered by the interference between the mixed D and D^* mesons.

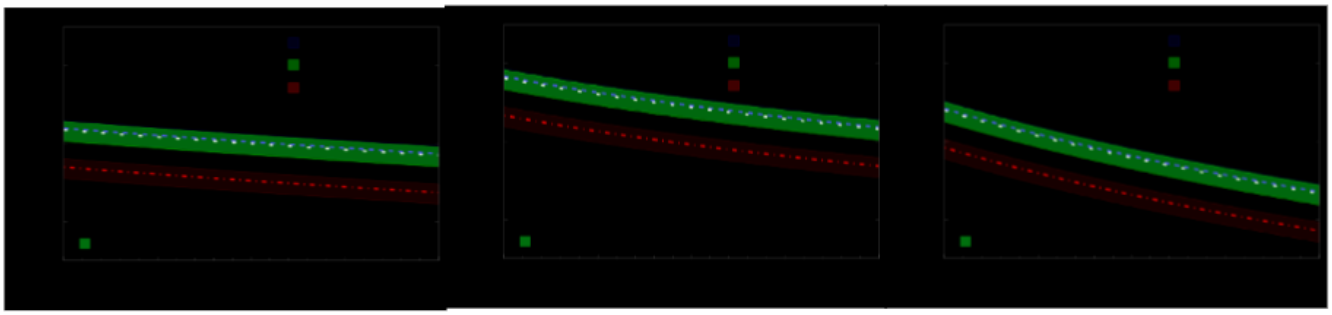

(a) (b) (c)

Figure 9 Differential cross section $d\sigma/dt$ for $\bar{p}p \to \Lambda_c\bar{\Sigma}_c^*$ at $p_{\text{lab}} = 15\ \text{GeV}/c$ versus $t_{\text{max}} - t$ for F, F_1, F_2. The conserving and violating parts contribute about 90% and 10%, respectively. This corresponds to the final state for the production of the charmed baryon triplet Σ_c^* ($J^P = 3/2^+$) and the charmed baryon singlet Λ_c ($J^P = 1/2^+$).

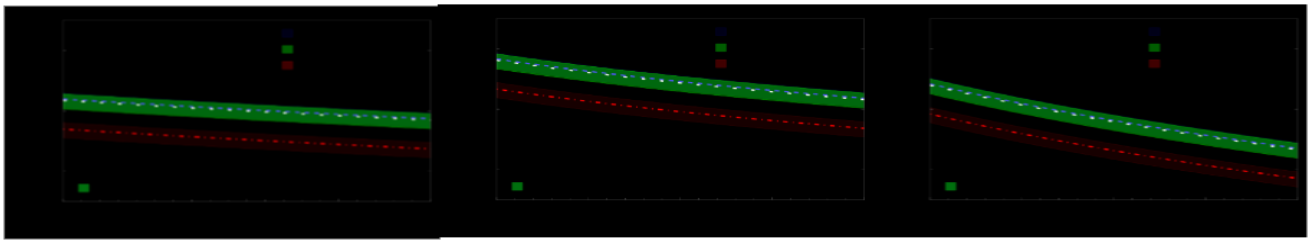

Figure 10 Differential cross section $d\sigma/dt$ for $\bar{p}p \to \Sigma_c^* \bar{\Lambda}_c$ (charge-conjugate ordering of **Figure 9**) at $p_{\text{lab}} = 15\ \text{GeV}/c$ versus $t_{\text{max}} - t$ for F, F_1, F_2. The conserving and violating parts contribute about 90% and 10%, respectively. This corresponds to the final state for the production of the charmed baryon triplet Σ_c^* ($J^P = 3/2^+$) and the charmed baryon singlet Λ_c ($J^P = 1/2^+$).

The production rates for the charmed baryon triplet Σ_c^* ($J^P = 3/2^+$) and the charmed baryon singlet Λ_c ($J^P = 1/2^+$) in the processes $p\bar{p} \to \Sigma_c^* \bar{\Lambda}_c, \Lambda_c \bar{\Sigma}_c^*$ are calculated, as depicted in **Figures 9** and **10**. The conserving term is dominant primary at 90%, falling within the range 10^{-4}-$10^{-2}\ \mu\text{b}/\text{GeV}^2$, with estimated as $10^{-4}(F)$, $10^{-2}(F_1)$ and $10^{-3}(F_2)$ $\mu\text{b}/\text{GeV}^2$. Notice that the percents coincidentally matches the level observed in the processes $\Sigma_c^* \bar{\Sigma}_c$ and $\Sigma_c \bar{\Sigma}_c^*$. However, the rates for F_1 and F_2 are about ten times larger compared to those processes, while F remains unchanged at the order of $10^{-4}\mu\text{b}/\text{GeV}^2$. These proportions are equal due to a well-defined ratio in the CHQSS and VHQSS Lagrangians, as shown in Eqs. (14) - (15), combined with the spin-averaged and spin-summed amplitude for the final-state particles, which leads to near decimal-level cancellation. Among the form factors, F_1 consistently displays the highest peak.

B. Comparison results with previous studies of the charmed baryon productions

In this subsection, we calculate the total cross-sections, σ_{total} and compare with previous studies, focusing on different $p_{\text{Lab}}(\text{GeV}/c)$ thresholds, as illustrated in **Table 1**.

Table 1 Total cross-sections (σ_{total}) for different channels in the $p\bar{p} \to Y_c \bar{Y}'_c$ process.

	Total Cross-Section (σ_{total}) (μb)				
$p\bar{p} \to Y_c \bar{Y}'_c$	**Quark-gluon String model [10]**	**Effective Lagrangian model [16]**	**Kaidalov's QGSM [12]**	**Quark-gluon dynamics [15]**	**This study**
$\Lambda_c \bar{\Lambda}_c$ (10.5 GeV/c)	1.03×10^{-2}	3.2×10^{-3}	$(1.98 - 28.2) \times 10^{-2}$	$1.94 - 3.07$	$(0.20 - 1.50) \times 10^{-3}$ (F) $(1.77 - 5.68) \times 10^{-3}$ (F_1) $(0.41 - 1.31) \times 10^{-4}$ (F_2)
$\Sigma_c \bar{\Sigma}_c$ (12 GeV/c)	-	-	$(1.07 - 60.2) \times 10^{-3}$	$(4.92 - 9.68) \times 10^{-4}$	$(1.13 - 3.61) \times 10^{-4}$ (F) $(2.53 - 8.08) \times 10^{-4}$ (F_1) $(2.31 - 7.38) \times 10^{-6}$ (F_2)
$\Sigma_c \bar{\Lambda}_c$ (11 GeV/c)	-	-	$(5.05 - 136) \times 10^{-3}$	$(5.09 - 9.83) \times 10^{-3}$	$(0.69 - 5.02) \times 10^{-4}$ (F) $(3.04 - 9.74) \times 10^{-4}$ (F_1) $(2.15 - 6.87) \times 10^{-6}$ (F_2)
$\Sigma_c^* \bar{\Sigma}_c^*$ (15 GeV/c)	-	-	-	-	$(1.99 - 6.39) \times 10^{-4}$ (F) $(6.73 - 21.51) \times 10^{-4}$ (F_1) $(0.02 - 6.48) \times 10^{-4}$ (F_2)

Our predicted total cross-sections for the reaction $\Lambda_c\overline{\Lambda}_c$ for each form factor at $p_{\text{Lab}} = 10.5\ \text{GeV}/c$ fall within the range of $10^{-4} - 10^{-3}\ \mu\text{b}$. In spite of structural differences in the form factors and couplings, as studied in Ref. [16], which is based on an effective Lagrangian model, our results remain consistent for F and F_1. This indicates that the inclusion of all super-multiplet fields in CHQSS and VHQSS leads to reliable predictions. However, they are about 10 times lower than the results in Ref. [10], which are based on the non-perturbative QGSM and are in approximate agreement with Ref. [12], which employs Kaidalov's QGSM with Regge poles and uses strong couplings derived from QCD light-cone sum rules. In contrast, our results are approximately 1000 times smaller than those from Ref. [15], which investigates kinematic thresholds based on Quark-gluon dynamics. For F_2, the cross-sections deviate significantly, being more than 10 times smaller than those for the other form factors.

For $\Sigma_c\bar{\Sigma}_c$ production at $p_{\text{Lab}} = 12\ \text{GeV}/c$, we find that the cross-sections fall within the range of $10^{-6} - 10^{-4}\ \mu\text{b}$. These results are consistent with Ref. [15] which reports values on the order of $10^{-4}\ \mu\text{b}$ for the form factors F and F_1 and are also are lower than those in Ref. [12], with stronger suppression in the F_2 constraint. Moreover, the total cross-section σ_{total} shows a significant decrease compared to that for $\Lambda_c\overline{\Lambda}_c$, by about one to two orders of magnitude. For $\Sigma_c\overline{\Lambda}_c$ production at a laboratory momentum of $11\ \text{GeV}/c$, our predictions lie in the range of 10^{-6} to $10^{-4}\ \mu\text{b}$. These results are smaller than those reported in Refs. [12,15] by about one to three orders of magnitude. These trends are similar to those for $\Sigma_c\bar{\Sigma}_c$, but slightly higher.

Note that, as discussed earlier, as t increases, F_2 becomes more suppressed, which should be carefully considered. This suppression is evident in the $d\sigma/dt$ results, despite equal values at $t_{\text{max}} - t = 0$. Finally, we have predicted σ_{total} for the reaction $p\bar{p} \to \Sigma_c^*\bar{\Sigma}_c^*$ at $p_{\text{Lab}} = 15\ \text{GeV}/c$. Our observations are $(1.99 - 6.39) \times 10^{-4}\ \mu\text{b}$ (F), $(6.73 - 21.51) \times 10^{-4}\ \mu\text{b}$ (F_1) and $(0.02 - 6.48) \times 10^{-4}\ \mu\text{b}$ (F_2) respectively. Since this process has not been extensively studied, no existing model is available for comparison.

Conclusions

In this work, we constructed the CHQSS and VHQSS Lagrangians under HQSS $SU(2)_v$ transformations. These Lagrangians reveal the proportions of conserving and violating couplings for pseudoscalar and axial-vector interactions. As in Refs. [20,23], these implications reduce parameters, enabling estimation of unknown LECs. The vertex coupling constants are adopted from Ref. [17], incorporating $SU(4)_f$ symmetry breaking with a deviation of about 20% relative to $SU(3)_f$ symmetry. Moreover, we investigated $d\sigma/dt$ for charmed production processes and evaluated the contributions from HQSS and its violation. As a result, the conserving contribution is slightly smaller than the violation average, with 47% for $\Lambda_c\overline{\Lambda}_c$. In contrast, the conserving parts are higher, with 66% for $\Sigma_c\bar{\Sigma}_c$ and 90% for $\Sigma_c^*\bar{\Sigma}_c$ and $\Sigma_c\bar{\Sigma}_c^*$, with $\Sigma_c^*\bar{\Sigma}_c^*$ being the most dominant at 98%. These results indicate that conserving HQSS works well when particles have heavy-quark spin partners, while more HQSS breaking effects appear in $\Lambda_c\overline{\Lambda}_c$ and appears weaker in excited charmed baryons.

The $d\sigma/dt$ for $p\bar{p} \to \Lambda_c\overline{\Lambda}_c$ and $\Sigma_c\bar{\Sigma}_c$, varies between $10^{-3} - 10^{-1}\ \mu\text{b}/\text{GeV}^2$ and $10^{-3} - 10^{-2}\ \mu\text{b}/\text{GeV}^2$ respectively, which is consistent with the results reported in Refs. [11,12] for form factor F and F_2. The ratio of the conserving contributions in $\Sigma_c^*\bar{\Sigma}_c^*$ and $\Sigma_c^*\bar{\Sigma}_c(\Sigma_c\bar{\Sigma}_c^*)$ is of the same order, 10^{-4}–$10^{-3}\ \mu\text{b}/\text{GeV}^2$. However, the production of $\Sigma_c^*\bar{\Sigma}_c^*$ is clearly smaller by about a factor of 10 compared to the violating contributions. Furthermore, they indicate that as t increases, the form factor F_2 induces stronger suppression.

We also presented the predicted σ_{total} for $\Lambda_c\overline{\Lambda}_c$ at $p_{\text{Lab}} = 10.5\ \text{GeV}/c$, estimated to be in the range of $10^{-4} - 10^{-3}\ \mu\text{b}$, in close agreement with previous studies in Refs. [16], which similar to our framework. For $\Sigma_c\bar{\Sigma}_c$ at $p_{\text{Lab}} = 12\ \text{GeV}/c$, the constrained form factors F and F_1 agree with those in Ref. [15]. In contrast, $\Sigma_c\overline{\Lambda}_c$ decreases by factors of 10 and 1000 compared to the results reported in Refs. [12,15]. Additionally, we computed σ_{total} for $\Sigma_c^*\bar{\Sigma}_c^*$ at $p_{\text{Lab}} = 15\ \text{GeV}/c$, with results presented around $10^{-4}\ \mu\text{b}$ for all form factors. As mentioned before, this work and previous studies provide model-dependent

charm production predictions that vary widely but still offer insight for guiding experiments.

For the forthcoming $\overline{\text{P}}$ANDA experiments at FAIR, the High-Energy Storage Ring (HESR) will store antiprotons in a momentum range from 1.5 to 15 GeV/c [40,33]. Hopefully, our results will provide in exploring the nature of charmed baryons and also serve as the first step towards more involved reaction mechanisms, leading to an increase in experimental requirements.

Acknowledgements

NM. is financially supported by Development and Promotion of Science and Technology Talents Project (DPST), Thai government scholarship. N.P. is financially supported by the National Astronomical Research Institute of Thailand (NARIT). A.J.A. was supported by RIKEN special postdoctoral researcher program. D.S. is supported by the Fundamental Fund of Khon Kaen University and has received funding support from the National Science, Research and Innovation Fund and supported by Thailand NSRF via PMU-B [grant number B39G680009].

Declaration of Generative AI in Scientific Writing

The authors acknowledge the use of the generative AI tool i.e., ChatGPT by OpenAI in the preparation of the manuscript, specifically for language editing and grammar correction. AI performed no content generation or data interpretation. The authors take full responsibility for the content and conclusions of this work.

CRediT Author Statement

Nantana Monkata: Investigation, Methodology, Calculation, Formal analysis, Validation, and Writing original draft. **Prin Sawasdipol:** Formal analysis, Conceptualization, Calculation, Software, and Validation. **Nongnapat Ponkhuha:** Investigation, Calculation, Validation, and Visualization. **Ratirat Suntharawirat:** Investigation, Calculation, Validation, and Visualization. **Ahmad Jafar Arifi:** Formal analysis, Conceptualization, Calculation, and Validation. **Daris Samart:** Conceptualization, Methodology, Project administration, Resources, Supervision, Funding acquisition, Validation, and Writing original draft.

References

[1] EG Cazzoli, AM Cnops, PL Connolly, RI Louttit, MJ Murtagh, RB Palmer, NP Samios, TT Tso and HH William. Evidence for $\Delta S = -\Delta Q$ Currents or Charmed Baryon Production by Neutrinos. *Physical Review Letters* 1975; **34**, 1125.

[2] W Chen, J Ho, TG Steele, RT Kleiv, B Bulthuis, D Harnett, T Richards and SL Zhu. *Exotic hadron states. In*: Proceedings of the 30th International Workshop on High Energy Physics: Particle and Astroparticle Physics, Gravitation and Cosmology: Predictions, Observations and New Projects, Protvino, Russia. 2014, p. 137-143.

[3] B Aubert, R Barate, D Boutigny, F Couderc, JM Gaillard, A Hicheur, Y Karyotakis, JP Lees, V Tisserand, A Zghiche, A Palano, A Pompili, JC Chen, ND Qi, G Rong, P Wang, YS Zhu, G Eigen, I Ofte, B Stugu, …, H Neal. Study of the $B \to J/\psi K^-\pi^+\pi^-$ decay and measurement of the $B \to X(3872)K^-$ branching fraction. *Physical Review Journals* 2005; **71**, 071103.

[4] B. Aubert, R Barate, D Boutigny, F Couderc1, Y Karyotakis1, JP Lees, V Poireau, V Tisserand, A Zghiche, E Grauges, A Palano, M Pappagallo, A Pompili, JC Chen, ND Qi, G Rong, P Wang, YS Zhu, G Eigen, I Ofte, B Stugu, GS Abrams, M Battaglia, AB Breon, DN Brown, J Button-Shafer, RN Cahn, E Charles, CT Day, …, H Neal. Observation of a broad structure in the $\pi^+\pi^- J/\psi$ mass spectrum around 4.26GeV/c^2 . *Physical Review Letters* 2005; **95**, 142001.

[5] K Abe, I Adachi, H Aihara, K Arinstein, Y Asano, V Aulchenko, T Aushev, T Aziz, AM Bakich, V Balagura, M Barbero, I Bedny, U Bitenc, I Bizjak, A Bondar, M Bracko, J Brodzicka, TE Browder, Y Chao, A Chen, BG Cheon, R Chistov, SK Choi, Y Choi, YK Choi, A Chuvikov, S Cole, …, J Dalseno. Observation of a new charmonium state in double charmonium production in e^+e^- annihilation at $\sqrt{s} \approx 10.6 - \text{GeV}$. *Physical Review Letters* 2007; **98**, 082001.

[6] SK Choi, SL Olsen, K Abe, T Abe, I Adachi, BS Ahn, H Aihara, K Akai, M Akatsu, M Akemoto, Y

Asano, T Aso, V Aulchenko, T Aushev, AM Bakich, Y Ban, S Banerjee, A Bondar, A Bozek, M Bračko, …, J Brodzicka. Observation of a narrow charmonium-like state in exclusive $B^{\pm} \to K^{\pm}\pi^{+}\pi^{-}J/\psi$ decays. *Physical Review Letters* 2003; **91**, 262001.

[7] SK Choi, SL Olsen, I Adachi, H Aihara, V Aulchenko, T Aushev, T Aziz, AM Bakich, V Balagura, I Bedny, U Bitenc, A Bondar, A Bozek, M Bračko, J Brodzicka, TE Browder, P Chang, Y Chao, A Chen, KF Chen, …, WT Chen. Observation of a resonance-like structure in the $\pi^{\pm}\psi'$ mass distribution in exclusive $B \to K\pi^{\pm}\psi'$ decays. *Physical Review Letters* 2008; **100**, 142001.

[8] R Aaij, CA Beteta, B Adeva, M Adinolfi, C Adrover, A Affolder, Z Ajaltouni, J Albrecht, F Alessio, M Alexander, S Ali, G Alkhazov, PA Cartelle, AA Alves, S Amato, S Amerio, Y Amhis, L Anderlini, J Anderson, R Andreassen, …, RB Appleby. Determination of the X (3872) meson quantum numbers. *Physical Review Letters* 2013; **110**, 222001.

[9] R Aaij, B Adeva, M Adinolfi, A Affolder, Z Ajaltouni, J Albrecht, F Alessio, M Alexander, S Al, G Alkhazov, PA Cartelle, AA Alves, S Amato, S Amerio, Y Amhis, L An, L Anderlini, J Anderson, R Andreassen, M Andreotti, …, A Zvyagin. Observation of the resonant character of the $Z(4430)^{-}$state. *Physical Review Letters* 2014; **112**, 222002.

[10] AB Kaidalov and PE Volkovitsky. Binary reactions in $\bar{p}p$ collisions at intermediateenergies. *Zeitschrift für Physik C Particles and Fields* 1994; **63**, 517-524.

[11] AI Titov and B Kampfer. Exclusive charm production in $\bar{p}p$ collisions at $\sqrt{s} \lesssim 15$ GeV. *Physical Review C* 2008; **78**, 025201.

[12] A Khodjamirian, C Klein, T Mannel,and YM Wang. How much charm can PANDA produce? *The European Physical Journal A* 2012; **48**, 31.

[13] J Haidenbauer and G Krein. Charm production in antiproton-proton annihilation. *Few-Body Systems* 2011; **50**, 183-186.

[14] J Haidenbauer and G Krein. The Reaction $p\bar{p} \to \bar{\Lambda}_c\Lambda_c^{+}$ close to threshold. *Physics Letters B* 2010; **687(4-5)**, 314-319.

[15] J Haidenbauer and G Krein. Production of charmed baryons in $\bar{p}p$ collisions close to their thresholds. *Physical Review D* 2017; **95**, 014017.

[16] R Shyam and H Lenske. Reaction $\bar{p}p \to \bar{\Lambda}_c^{-}\Lambda_c^{+}$within an effective lagrangian model. *Physical Review D* 2014; **90**, 014017.

[17] T Sangkhakrit, SI Shim, Y Yan and A Hosaka. Charmed baryon pair production in proton-antiproton collisions in effective Lagrangian and Regge approaches. *The European Physical Journal A* 2022; **58**, 32.

[18] ML Du, E Hernández and J Nieves. Is the $\Lambda_c(2625)^{+}$the heavy quark spin symmetry partner of the $\Lambda_c(2595)^{+}$?. *Physical Review D* 2022; **106(11)**, 114020.

[19] V Baru, E Epelbaum, AA Filin, C Hanhart and AV Nefediev. Emergence of heavy quark spin symmetry breaking in heavy quarkonium decays. *Physical Review D* 2023; **107**, 014027.

[20] D Samart, C Nualchimplee and Y Yan. Combined heavy-quark symmetry and large N_c operator analysis for 2-body counterterms in the chiral Lagrangian with D mesons and charmed baryons. *Physical Review D* 2016; **93**, 116004.

[21] V Baru, E Epelbaum, AA Filin, C Hanhart and AV Nefediev. Heavy-quark spin symmetry partners of the $X(3872)$ molecule. *JPS Conference Proceedings* 2017; **13**, 020023.

[22] O Romanets, L Tolos, C García-Recio, J Nieves, LL Salcedo and R Timmermans. Heavy-quark spin symmetry for charmed and strange baryon resonances. *Nuclear Physics A* 2013; **914**, 488-493.

[23] MFM Lutz, D Samart and A Semke. Combined large- N_c and heavy-quark operator analysis of 2-body meson-baryon counterterms in the chiral Lagrangian with charmed mesons. *Physical Review D* 2011; **84**, 096015.

[24] JM Suh and HC Kim. Axial-vector transition form factors of the singly heavy baryons. *Physical Review D* 2022; **106**, 094028.

[25] JY Kim and HC Kim. Electromagnetic form factors

of singly heavy baryons in the self-consistent SU(3) chiral quark-soliton model. *Physical Review D* 2018; **97(11)**, 114009.

[26] F Hussain and G Thompson. *An Introduction to the heavy quark effective theory*. *In*: E Gava, A Masiero, KS Narain, S Randjbar-Daemi and Q Shafi (Eds.). Proceedings, summer school in high-energy physics and cosmology: Trieste, Italy, June 13-July 29, 1994. ICTP Summer School in High-energy Physics and Cosmology, Trieste, 1995, p. 0045-0115.

[27] A Belyaev. *Nuclei and particles.* University of Southampton, Southampton, United Kingdom.

[28] DR Entem, PG Ortega and F Fernandez. Partners of the $X(3872)$ and HQSS breaking. *In*: MR Pennington (Ed.). Proceedings, 16th International conference on hadron spectroscopy (Hadron 2015): Newport News, Virginia, USA, September 13-18, 2015. AIP Conference Proceedings, New York, 2016, p. 060006.

[29] W Qin, SR Xue and Q Zhao. Production of $Y(4260)$ as a hadronic molecule state of $\bar{D}D_1 +$ c.c. in e^+e^- annihilations. *Physical Review D* 2016; **94**, 054035.

[30] D Skoupil and Y Yamaguchi. Photoproduction of $\bar{D}^0\Lambda_c^+$ within the Regge-plusresonance model. *Physical Review D* 2020; **102**, 074009.

[31] G Krein. SU(4)-flavor symmetry breaking in hadron couplings. *In*: Proceedings of science, Trieste, Italy. 2012, p. 144.

[32] CE Fontoura, J Haidenbauer and G Krein. $SU(4)$ flavor symmetry breaking in D meson couplings to light hadrons. *The European Physical Journal A* 2017; **53**, 92.

[33] W Erni, I Keshelashvili, B Krusche, M Steinacher, Y Heng, Z Liu, H Liu, X Shen, O Wang, H Xu, J Becker, F Feldbauer, FH Heinsius, T Held, H Koch, B Kopf, C Motzko, M Peliz¨aus, B Roth, T Schr¨oder, …, R Timmermans. *Physics performance report for PANDA: Strong interaction studies with antiprotons.* 2009.

[34] S Sakai, HJ Jing and FK Guo. Decays of P_c into $J/\psi N$ and $\eta_c N$ with heavy quark spin symmetry. *Physical Review D* 2019; **100**, 074007.

[35] J Haidenbauer and G Krein. Production of charmed pseudoscalar mesons in antiproton-proton annihilation. *Physical Review D* 2014; **89**, 114003.

[36] R Shyam and K Tsushima. Production of Λ_c^+ hypernuclei in antiproton - nucleus collisions. *Physics Letters B* 2017; **770**, 236-241.

[37] R Shyam. Charmed-baryon production in antiproton-proton collisions within an effective Lagrangian model. *Physical Review D* 2017; **96**, 116019.

[38] AT Goritschnig, P Kroll and W Schweiger. Proton-antiproton annihilation into a $\Lambda_c^+\bar{\Lambda}_c^-$ Pair. *The European Physical Journal A* 2009; **42**, 43-62.

[39] D Iglesias-Ferrero, DR Entem, F Fernández and PG Ortega. Production of singlecharmed baryons in a quark model approach. *Physical Review D* 2022; **106**, 094027.

[40] L Frankfurt, M Strikman, A Larionov, A Lehrach, R Maier, HV Hees, C Spieles, V Vovchenko and H Stoecker. PANDA as midrapidity detector for a future HESR collider at FAIR. *The European Physical Journal A* 2020; **56**, 171.